

Detecting Inception of Hydrodynamic Cavitation Noise of Ships using Quadratic Phase Coupling Index as an Indicator

M. Sandhya*, K. Rajarajeswari#, and P. Seetaramaiah@

*Naval Science and Technological Laboratory, Visakhapatnam-530 027, India

#VITAM College of Engineering, Visakhapatnam- 531 173, India

@Andhra University, Visakhapatnam-530 003, India

*E-mail: sanmsms@yahoo.co.in

ABSTRACT

There is ever increasing interest in underwater noise control onboard ships as part of concerted efforts to reduce ship's radiated noise. Reduction of radiated noise is considered important as it will affect the performance of hydro-acoustic systems such as sonars, echo sounders, towed systems, etc. Out of three major sources of noise onboard ships, viz., machinery, propeller, and hydrodynamic noise, propeller noise is considered a major source beyond certain speed at which propellers cavitate produces cavitation noise. The inception speed of propeller cavitation is generally accompanied by sudden increase in radiated noise level of 8-15 dB when measured using a hydrophone placed on the seabed. This paper attempts to establish the concept of quadratic phase coupling index as an indicator to detect inception of cavitation of ship propellers. This concept was tested on actual ship radiated noise data measured at sea for evaluating its effectiveness.

Keywords: Marine propellers, cavitation, bispectrum, bicoherence, higher order spectra, radiated noise, quadratic phase coupling

NOMENCLATURE

P	: Pressure
P_{LO}	: Equilibrium pressure in the liquid
P_v	: Vapour pressure
P_m	: Minimum pressure
R	: Radius of the cavitating bubble
R_o	: Maximum bubble radius
T_e	: Expansion time of bubble
T_c	: Collapse time of bubble
$T_b = T_e + T_c$: Bubble life time
B_{yx}	: Cross-bispectrum
b_{xx}	: Auto-bicoherence
f	: Frequency

1. INTRODUCTION

Underwater radiated noise from merchant ships or naval vessels is mainly due to three major sources¹, viz., machinery, propeller, and hydrodynamic interaction. Machinery noise is known to be dominant source when the ships are sailing at low speeds. Though propeller and hydrodynamic interaction produces noise, these are not considered dominant at low speeds (up to 10-12 knots in case of typical warships). As speed of the vessel increases further, propeller noise due to cavitation becomes dominant over machinery noise. Hydrodynamic noise becomes dominant over various other noises at relatively high speeds (beyond 20 knots for typical warship). Propeller cavitation is generally accompanied

by sudden increase in noise level, as much as 8 dB - 15 dB or even more, when compared to non-cavitating state. By measuring increase in propeller cavitating noise level, one can judge whether propeller is cavitating or not. This paper proposes another indicator of cavitation inception namely quadratic phase coupling (QPC) Index based on the data measured during a ship noise measurement experiment.

The cavitation noise radiated from a cavitating propeller which occurs above certain revolutions per minute (rpm), consists of contributions from various sources like variation in cavitation volume and shape, skin friction noise on the blade, variation in the thrust and propeller loading. Of these sources, fluctuating volume of the individual bubbles may be regarded as a monopole source with highest radiation efficiency.

The cavitation bubbles thus generated out of the in-trapped air on the propeller blade generally pass through a pressure well induced by the propeller where the pressure may drop below the vapour pressure. This causes the bubble to expand in volume followed by a rapid reduction of the volume, as shown in Figs. 1(a) and 1(b)². The collapse of bubbles caused by cavitation process produces intense local heating and high pressures with very short lifetimes. The collapse of bubbles in a multi-bubble cavitation field produces hot spots with effective temperatures of ~5000 °K, pressure of ~1000 atmospheres, and heating-cooling rates above 10¹⁰ K/s.

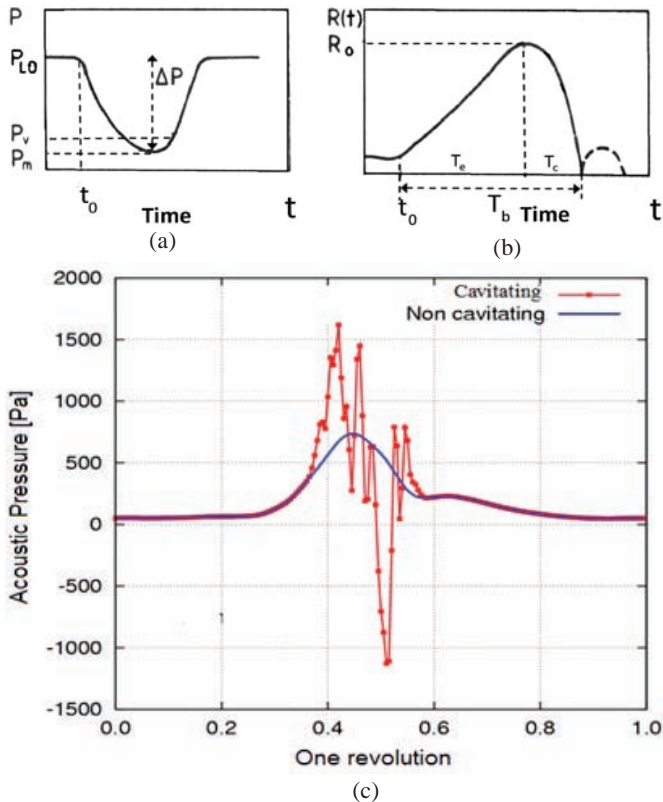


Figure 1. (a) Cavitation pressure, and (b) bubble radius variation as a function of time, and (c) Variation in propeller blade pressure in non-cavitating and cavitating conditions over one rpm.

Thus cavitation can create extraordinary physical and chemical conditions in otherwise cold liquids³. Cavity collapse near an extended solid surface like propeller blade becomes non-spherical, drives high speed jets of liquid into the surface and creates shockwave damage to the surface⁴. A shockwave emitting from the collapse of individual bubbles constitutes a white random noise source. This process can produce newly exposed, highly heated surfaces, and is responsible for the erosion, corrosion and intense radiated noise problems associated with hydrodynamic cavitation of ships propellers. It is reported in the literature that the size of cavitation bubbles can vary from 100 nm to 3 mm in diameter.

Figure 1(c) shows a theoretically computed single-blade pressure signal in non-cavitating and cavitating conditions at cavitation no. 3.645, as perceived by a hydrophone⁵. The time-domain signal under cavitating conditions is highly transient with several peaks, showing large fluctuations in pressure compared to the signal under non-cavitating conditions, amounting to nonlinear and non-Gaussian nature of signals over short periods. Sudden increase in overall acoustic pressure level is one indication of ship propeller cavitation due to such transient phenomenon in cavitating condition.

In the case of background noise and low-intensity cavitation noise, different spectral components of noise have a random phase relationship. If the cavitation noise intensity is sufficiently high, the nonlinear terms in the acoustic wave equation cannot be ignored; and these nonlinear

terms cause nonlinear interactions among different spectral components of cavitation noise. The dominant nonlinear interaction is the second-order interaction. Second-order interaction between components of frequencies f_1 and f_2 leads to the generation of components of frequencies $f_1 \pm f_2$ whose phases are coupled to the phases of the parent components. Presence of quadratic phase coupling can be detected by higher order spectral estimation techniques. Detection and quantification of the second-order or quadratic-phase coupling would be an effective way of detecting the onset of cavitation.

In statistical signal processing, third-order statistics, namely bispectrum and bicoherence are used to detect the quadratic nonlinearities. Use of bispectrum and bicoherence for analysis of ship radiated noise has been in practice for long. Bispectral analysis of ocean noise by Brockett⁶, *et al.* revealed that it is ‘linear and Gaussian’ when examined over longer periods (order of min.) but ‘nonlinear and non-Gaussian’ over shorter periods (order of sec.) as well as when signal was dominated by shipping noise. Hinich⁷, *et al.* carried out bispectral analysis of ship-radiated noise and showed that bispectrum could be used to indicate the existence of noise generating mechanisms which are normally hidden in the background noise. Richardson and Hodgkiss⁸ have used the bispectrum and bicoherence to analyse the underwater acoustic data and demonstrated that the bispectrum estimate can be used to detect non-Gaussianity, nonlinearity and harmonic coupling. Regazzoni⁹, *et al.* have used bispectrum to statistically characterise shipping noise and also to design a bispectrum based detector. Yu¹⁰, *et al.* have proposed a new feature vector and classification based on bispectrum for underwater targets.

QPC is a metric derived from the third-order statistics. Authors have proposed the applicability of the concept of QPC Index ($QPC I_n$), which was initially proposed by Srinivasan¹¹, *et al.* to quantify the coupling of complex twin-jet plumes of closely-spaced screech sources, as an alternative metric which can distinguish between two states of propeller cavitation, i.e., non-cavitating (NC) and cavitating (C) states. For the purpose of evaluating the QPC Index concept, the authors have considered underwater noise data of a typical ship with and without propeller cavitation.

2. MEASUREMENT OF SHIP PROPELLER CAVITATION NOISE

The acoustic signature of a typical ship required for establishing the concept based on QPC Index has been measured using a hydrophone placed on seabed. The ship was made to pass over the hydrophone at cavitating and non-cavitating speeds using marker buoys on either side of hydrophone for ship’s transit. The acoustic signature recording was started and stopped at the time when the ship was at 160 m. (approx) on either side of the hydrophone during ship’s transit (Fig. 2). Law of spherical spreading was used to compute the sound pressure level at 1m. distance¹². To avoid any filtering effect imposed

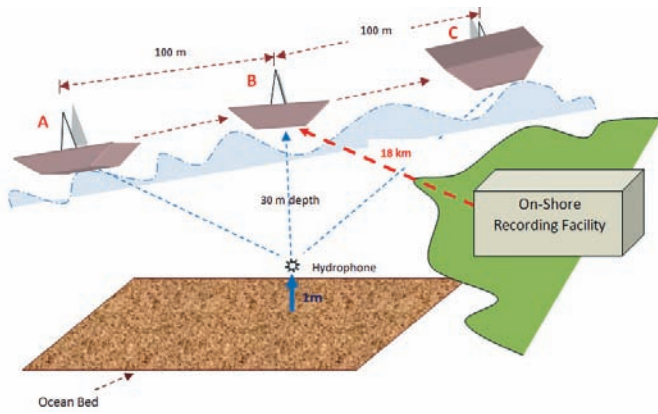


Figure 2. Sketch of noise measuring range.

by sea water, measurement was made at relatively close range to the extent possible, considering the fact that higher frequency components undergo greater attenuation since the absorption coefficient increases with frequency. The water depth is about 30 m. and the sea bottom is found to be soft mud which provides minimum reflection. The noise range data was acquired using a dedicated

data acquisition system (DAS) with wide frequency response and sufficient dynamic range placed far from the hydrophone connected by entrenched underwater cable. The complete digitized raw data has been stored in a dedicated computer system for future reference. Radiated noise spectra were computed from the time domain data of the measured noise signal using FFT.

A sketch of the noise measuring range and different locations (A, B, and C) of the moving ship with reference to the hydrophone are also shown in Fig. 2. Time domain noise signal recorded during ship transiting above the hydrophone is shown in Figs. 3(a) and 3(b). It is obvious that the radiated noise level measured by the hydrophone is highest when the ship is at location B, which is the point of closest approach (CPA) of the ship with reference to the hydrophone on the seabed.

Time fluctuation of the amplitudes of the recorded acoustic signal causes time fluctuations of the spectrum pressure levels of the ship radiated underwater noise also. Figures 4(a) and 4(b) show spectrograms (i.e., frequency vs time vs amplitude) of the hydro-acoustic characteristics of the passing ship corresponding to NC

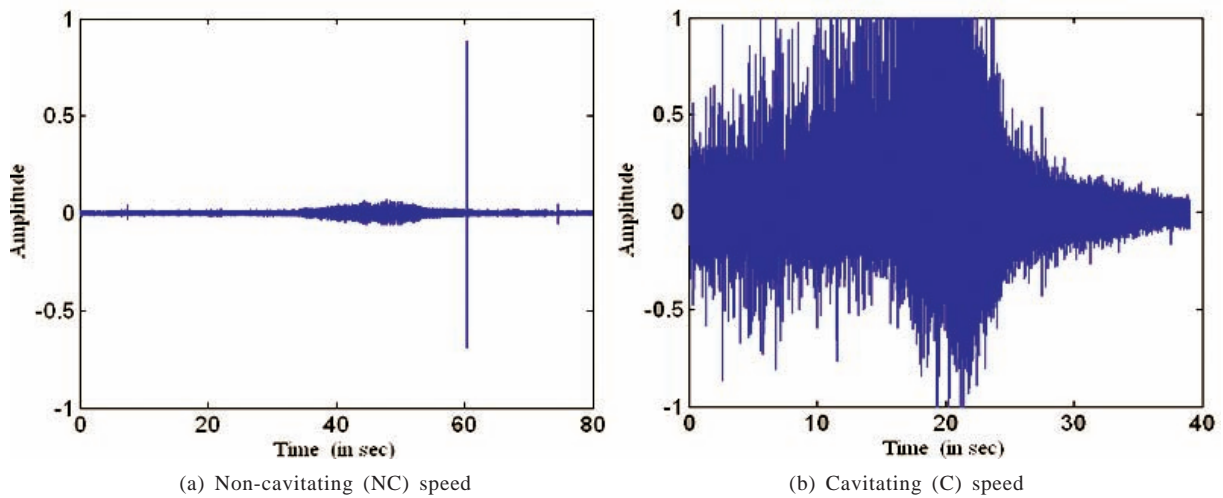


Figure 3. Noise signature of ship in time domain (sampling rate – 256 KHz).

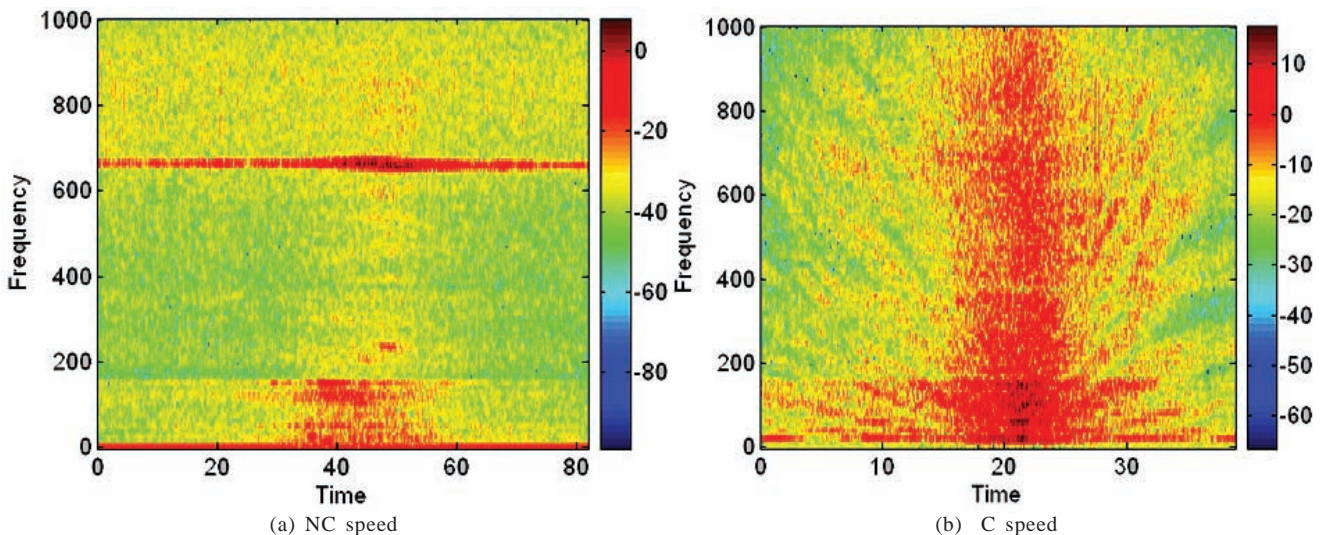


Figure 4. Acoustic spectrograms (0 KHz– 1 KHz) corresponding to Fig. 3(a) and 3(b).

and C speeds as at Figs. 3(a) and 3(b). Variation in the source receiver geometry influences the characteristics of the spectrogram of the radiated noise of the vessel during the ship's transit. On the basis of the recorded signal given in Fig. 3, it is reasonable to say that signal is the strongest during time period of about fifteen seconds when the ship is closest to the measuring hydrophone, or more exactly in the neighbourhood of CPA point. Signatures similar to those in Fig. 3 may be expected even when the measurements are made at greater distances, but the observed peak intensity levels would be lower due to propagation loss.

Based on propeller design data made available, measurements were carried out at two speeds of the vessel which represent two states of propeller noise. One characterises the non-cavitating state of propeller and the second, fully cavitating state of the propeller. The corresponding spectra of noise signatures at these speeds were observed to have very pronounced spectral components as shown in Fig. 5. In the low frequency band (0–50 Hz), a few tonal spectrum components marked as 1 to 8 exist with corresponding frequencies of 0.0916 Hz, 8.947 Hz, 17.47 Hz, 25.92 Hz, 34.66 Hz, 40.17 Hz, 49.22 Hz, and 62.34 Hz, respectively as shown in Fig. 6 which is a window of Fig. 5(a). The origins of spiky components are somewhat easy to identify as these are related to rpm of the machinery.

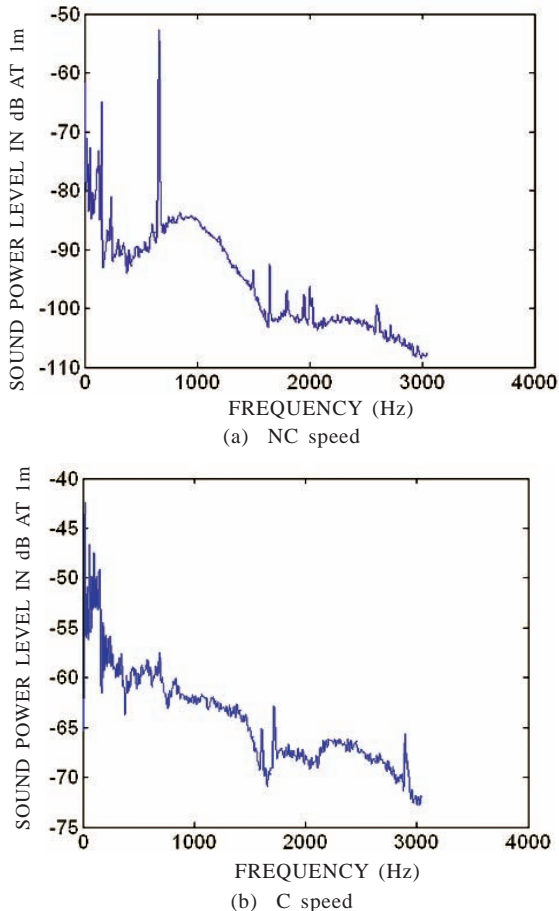


Figure 5. Power spectra corresponding to Figs. 3(a) and 3(b).

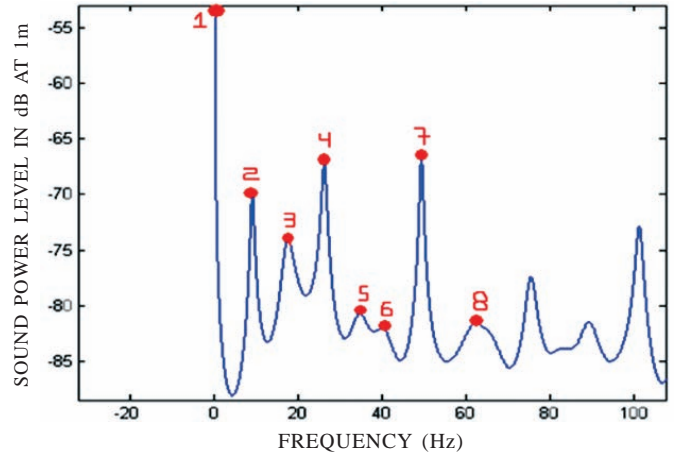


Figure 6. Low frequency components observed in the measured non-cavitating noise.

As the speed increases from NC to C, there is distinct change in the noise level and frequency content of noise signature. At C speed, most of the spiky components got drowned in the noise generated due to the cavitation phenomenon of propeller. At NC speed, the underwater noise was due to machinery running onboard rather than propeller cavitation. The propeller onboard the ship is expected to cavitate above a particular speed (varies for different classes of ships) which could not be avoided despite best design practices. That is the reason to measure the radiated noise at two different speeds, with and without propeller cavitation occurring. In this particular case, noise level itself could be used as indicator of cavitation inception. But in many other propellers, the noise level difference need not be a good indicator of cavitation inception. But this paper identifies how QPC index also could be used as indicator of cavitation inception.

3. LIMITATION OF CLASSICAL SPECTRAL ANALYSES OF SHIP RADIATED NOISE

Transformation of time-domain signals into the frequency domain-signals are performed using FFT. Stationary random process can be characterised by means of a spectral density function. This function provides information concerning the power as a function of frequency for the stationary process.

When dealing with actual physical phenomena and practical systems, the constraint about finite length record function is always present. For systems operating in real time, the record of interesting signals is limited in time domain. Therefore, practical spectral estimates must be limited to a finite frequency range.

It is felt that classical spectrum analysis should include windowing of the signal to be analysed. Many discrete time windows exist, such as, rectangle (uniform), triangle (Bartlett), raised cosine (Hamming), weighted cosine, etc. For the present analysis, Berg method users chosen.

Conventional digital signal processing is based on Fourier theory. By means of second-order power spectral analysis, only linear mechanisms can be studied since it

does not utilise the phase information which implies non-correlation among harmonic components. Power spectrum information is not sufficient to describe signals in case of non-Gaussianity and nonlinearity as is the case with propeller cavitation noise as shown in Fig. 1(c).

4. HIGHER ORDER SPECTRAL ANALYSES OF PROPELLER NOISE DATA

Higher order spectral (HOS) methods are generally used for understanding of nonlinear interactions among signals or among different components of a signal in many branches of engineering, resulting in several useful spectral tools for understanding nonlinear mechanism. In this study also, HOS tools are used to understand propeller cavitation noise, which is generated due to growth and collapse of water bubbles in an impulsive manner w.r.t time.

The autobispectrum and cross-bispectrum are nonlinear analogues of the auto spectrum and cross spectrum functions in the conventional linear spectral analysis. The auto- and crossbispectra are the Fourier Transform (FT) of triple time correlations of two functions of time, $x(t)$ and $y(t)$, the functions being identical in the case of autobispectrum. The mathematical form of cross-bispectrum is shown¹¹ in Eqn (1).

$$B_{yxx}(f_1, f_2) = \int_{-\infty}^{\infty} \int_{-\infty}^{\infty} \left[\lim_{T \rightarrow \infty} \int_{-T/2}^{T/2} y(t)x(t+\tau_1)x(t+\tau_2) dt \right] e^{-j2\pi(f_1\tau_1+f_2\tau_2)} d\tau_1 d\tau_2 \quad (1)$$

Another representation of cross-bispectrum in terms of the FTs is given in Eqn (2)

$$B_{yxx}(f_1, f_2) \equiv Y(f_1)X(f_2)X^*(f_1+f_2) \quad (2)$$

where $Y(f_1)$ and $X(f_2)$ are the FTs of the signals $y(t)$ and $x(t)$ evaluated at frequencies f_1 and f_2 respectively and $X^*(f_1+f_2)$ is the complex conjugate of the FT of signal $x(t)$ evaluated at frequency (f_1+f_2) .

The mathematical form of crossbicoherence is shown in Eqn (3)

$$b_{yxx}^2(f_1, f_2) = \frac{\left| \int_{-\infty}^{\infty} \int_{-\infty}^{\infty} \left[\lim_{T \rightarrow \infty} \int_{-T/2}^{T/2} y(t)x(t+\tau_1)x(t+\tau_2) dt \right] e^{-j2\pi(f_1\tau_1+f_2\tau_2)} d\tau_1 d\tau_2 \right|^2}{\left| \lim_{T \rightarrow \infty} \int_{-T/2}^{T/2} y(t)e^{-j2\pi f_1 t} dt \right|^2 \left| \lim_{T \rightarrow \infty} \int_{-T/2}^{T/2} x(t)e^{-j2\pi f_2 t} dt \right|^2 \left| \lim_{T \rightarrow \infty} \int_{-T/2}^{T/2} x(t)e^{-j2\pi(f_1+f_2)t} dt \right|^2} \quad (3)$$

Hence it can be seen that bicoherence is the normalized bispectrum.

It may be seen from Fig. 1(c) that the propeller noise due to growth and collapse of bubbles (implosions) is nonlinear and time-varying process, and the signatures of these nonlinear processes are measured using hydrophones placed on the seabed. Auto-bicoherence data obtained can be used to evaluate nonlinear interaction in both time and spatial domains.

The autobispectrum of a signal is a two-dimensional function of frequency and is generally complex-valued. In averaging over many ensembles (ref. 11, pg. 915), the magnitude of the autobispectrum will be determined by the presence (or absence) of a phase relationship among sets of the frequency components at f_1 , f_2 and $(f_1 + f_2)$ or at f_1 , f_2 and $(f_1 - f_2)$.

If there is a random phase relationship among these three components, the autobispectrum will average to a very small value. If the components are phase-locked, the corresponding autobispectrum will have a large magnitude.

Because a quadratic nonlinear interaction between two frequency components f_1 and f_2 yields a deterministic phase relationship between these and their summed component $(f_1 + f_2)$ or their difference component $(f_1 - f_2)$, the autobispectrum can be used to detect a quadratic coupling or interaction among different frequency components of a signal. The level of such coupling in a signal may be measured by estimating the bicoherence, $b_c^2(f_1, f_2)$ as shown in Eqn (4).

$$b_c^2(f_1, f_2) = \frac{\left| \sum_{k=1}^M X_k(f_1)X_k(f_2)X_k^*(f_1+f_2) \right|^2}{\sum_{k=1}^M |X_k(f_1)X_k(f_2)|^2 \sum_{k=1}^M |X_k^*(f_1+f_2)|^2} \quad (4)$$

where $X_k(f)$ is the DFT of the k^{th} sample of $x(t)$ and $X_k^*(f)$ the complex conjugate, evaluated at frequency f .

By the Schwarz inequality, the value of $b_c^2(f_1, f_2)$ varies between 0 and 1.

If there is no phase coupling, i.e., if there is a random phase relationship among the frequency components at f_1 , f_2 and $(f_1 + f_2)$ or $(f_1 - f_2)$, the value of the auto-bicoherence will be at or near zero (due to averaging effects)¹³.

If there is a phase coupling, there is a deterministic relationship among the frequency components at f_1 , f_2 and $(f_1 + f_2)$ or $(f_1 - f_2)$, then the value of the auto-bicoherence will be near unity. Values of the auto-bicoherence between zero and one indicate partial quadratic coupling.

5. METRICS PROPOSED TO EVALUATE PROPELLER CAVITATION

As the cavitation process sets in beyond certain hydrodynamic speed, both the magnitude and number of interactions between frequency components are expected to increase. The following fundamental frequency components and their harmonics are expected due to any propeller rotation which can be measured using a hydrophone¹⁴.

(i) Shaft frequency (Ns)

- (ii) Blade pass frequency ($Np = Ns \times \text{No. of blades}$)
- (iii) Blade natural frequency (N_N)

In any nonlinear dynamical system, there could be many possibilities of generating overtones from the above frequency components as ‘sum-interactions’ and ‘difference-interactions’. All these components are expected to be available in bicoherence spectra as and when this magnitude is detectable by the hydrophone.

To quantify the quadratic phase coupling with inception of cavitation, a metric called QPC In (Quadratic Phase Coupling index)¹¹ is shown in Eqn (5).

$$QPCI_n = \sum_{i=1}^N \sum_{j=1}^M \alpha(i, j) \quad (5)$$

where $\alpha(i, j)=1, b_c^2(f_i, f_j) \geq n = 0, b_c^2(f_i, f_j) < n$ where N and M are the no. of discrete frequency ranges in the bicoherence spectra, ‘ n ’ is the bicoherence threshold below which the uncertainties may clutter the analysis.

It can also be viewed as the interaction density. It is the number of peaks in the auto-bicoherence spectrum above a threshold value. QPC I_n can be estimated for different speeds of the propeller. As the propeller reaches from non-cavitation stage to cavitation stage, the QPC I_n will vary indicating different types of nonlinear interactions that exist as a function of propeller rpm in the cavitation noise generation process. QPC I_n will peak wherever number of phase couplings between signals emanated from any two bubbles in the cavitation zone maximise.

6. RESULTS AND DISCUSSIONS

Earlier studies have shown that there exists prominent bispectral components in the ship radiated noise where as the ambient noise does not have any significant bispectral components⁷.

The existence of a non-zero bispectrum indicates the existence of nonlinear interaction among the spectral components of noise. The bispectrum of noise could be used to indicate the existence of such noise sources as would normally be hidden in the background noise when the conventional spectral estimation procedures are adopted.

It can be surmised that, since the major effect of the nonlinearities is to cause intermodulations between the components of the driving process, without phase information, in addition to the spectral power, the presence of nonlinearities will not be detected.

The time domain underwater noise data was analysed using third-order spectra namely, bispectrum and bicoherence while using Rao-Gabr¹⁵ and Black man windows, respectively.

In the present study, sound pressure levels (SPL) show signatures from DC to 3 KHz range (Figs 5(a) and 5(b)). The radiated noise level increased by average 20 dB between NC and C speeds. The spiky components corresponding to rotating machinery seen at NC speed got drowned in the plot shown for C speed. C speed spectra are basically a broadband noise spectra. From

corresponding bispectrum plots Figs 7(a), 7(b), 8(a), and 8(b), it can be seen that there exist bispectral components without tonal components, but it is very difficult to relate the difference between the plots to cavitation in any quantitative form.

Corresponding bicoherence plots were plotted and shown in Figs 9 (a) and 9(b) and 10(a) to 10(d) for the same speeds. Again, it only indicates that bicoherence shows that partial coherence exists between innumerable frequencies. This is typical of cavitation noise which is nonlinear and is generated due to collapse of millions of bubbles as implosions. Relatively at NC speed, the bicoherence plot indicates less number of spiky components with relatively better coherence among various spiky components.

Bispectrum and bicoherence analysis up to 1 KHz and up to 3 KHz were carried out and QPC Index computed. Table 1 summarises the result for sum components of bispectrum analysis up to 1 KHz. Maximum and minimum thresholds were chosen at 95 % and 50 % approx. of maximum strength. We observed an order of 3.0e+3 (approx.) increase in the strength from NC state to the C state of cavitation. Also, an increase of 14 in QPC I_n was observed between the two states. However, QPC I_n remained the same at the maximum threshold value.

Table 2 presents QPC I_n values computed from bicoherence data using ‘sum’ components taken up to

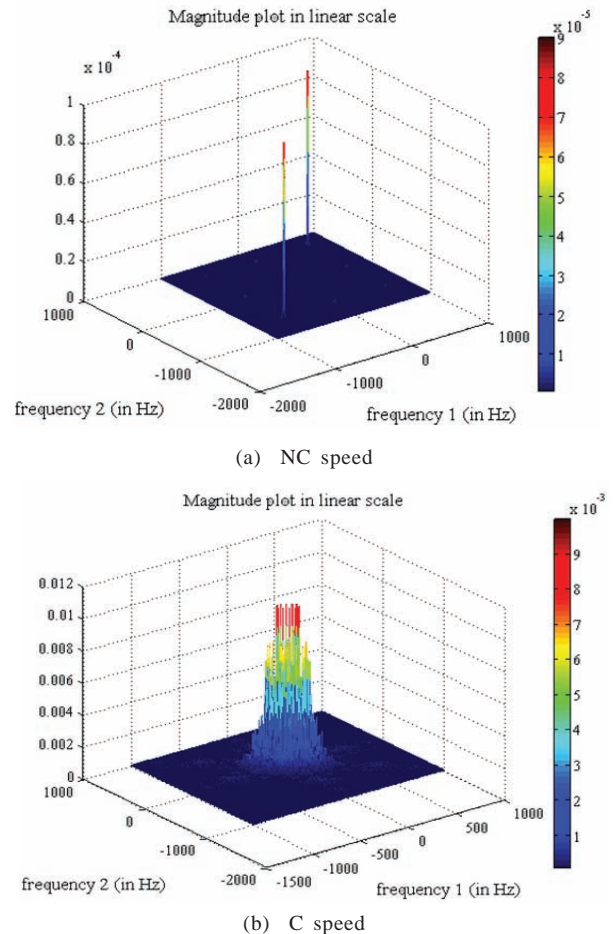


Figure 7. Bispectrum 0-1 KHz.

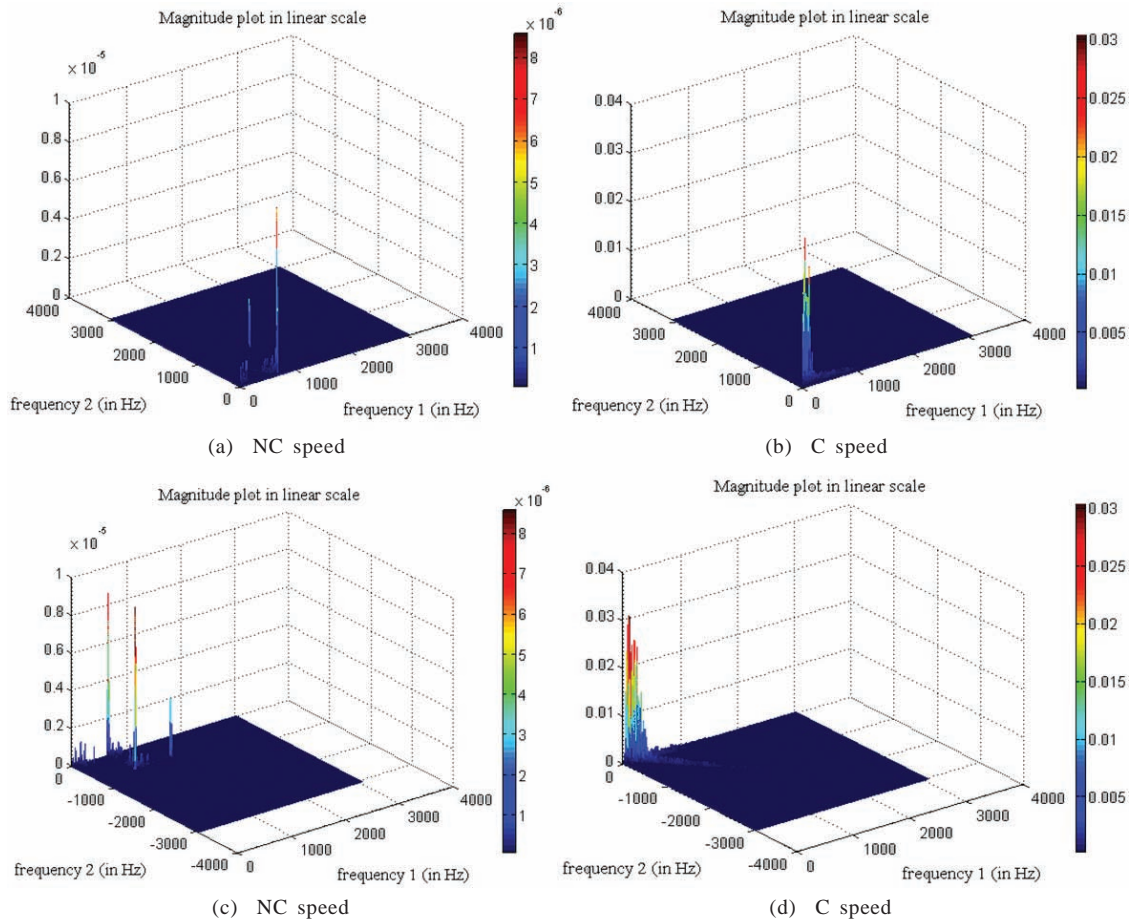


Figure 8. Bispectrum 0 - 3 KHz (a), (b) - sum components, (c), (d) - difference components.

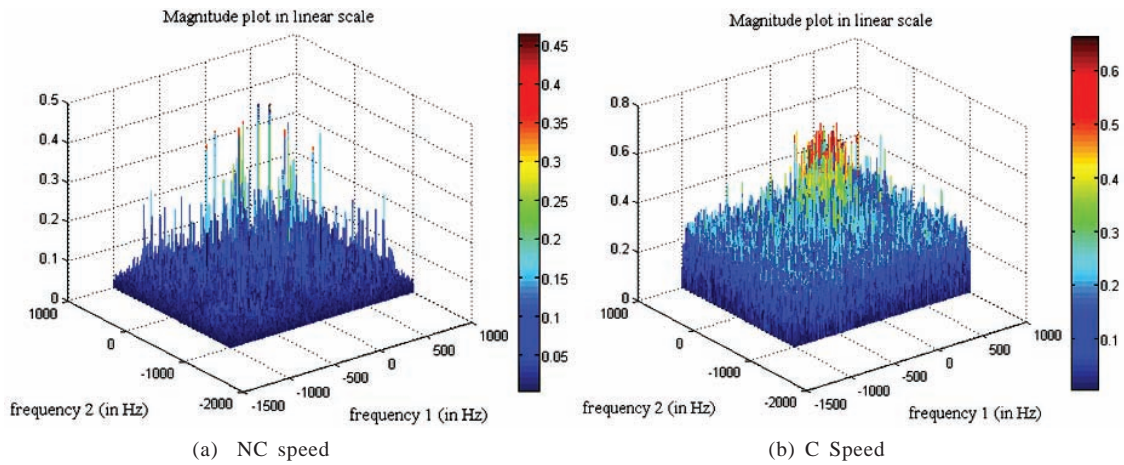


Figure 9. Bicoherence 0 – 1 KHz.

Table 1. QPC Index at maximum and minimum thresholds computed for two speeds of propeller noise obtained from sum components of bispectrum upto 1 KHz

Bispectrum	NC speed		C speed	
	Maximum	Minimum	Maximum	Minimum
Threshold value	3.0e-006	2.2e-006	9.0e-003	5.5e-003
QPC Index	1	4	1	18

Table 2. QPC Index at maximum and minimum thresholds computed for two speeds of propeller noise obtained from sum components of bi-coherence upto 1 KHz

Bi-coherence	NC speed		C speed	
Threshold value	Maximum	Minimum	Maximum	Minimum
	2.4e-001	1.5e-001	6.0e-001	4.0e-001
QPC Index	2	16	6	110

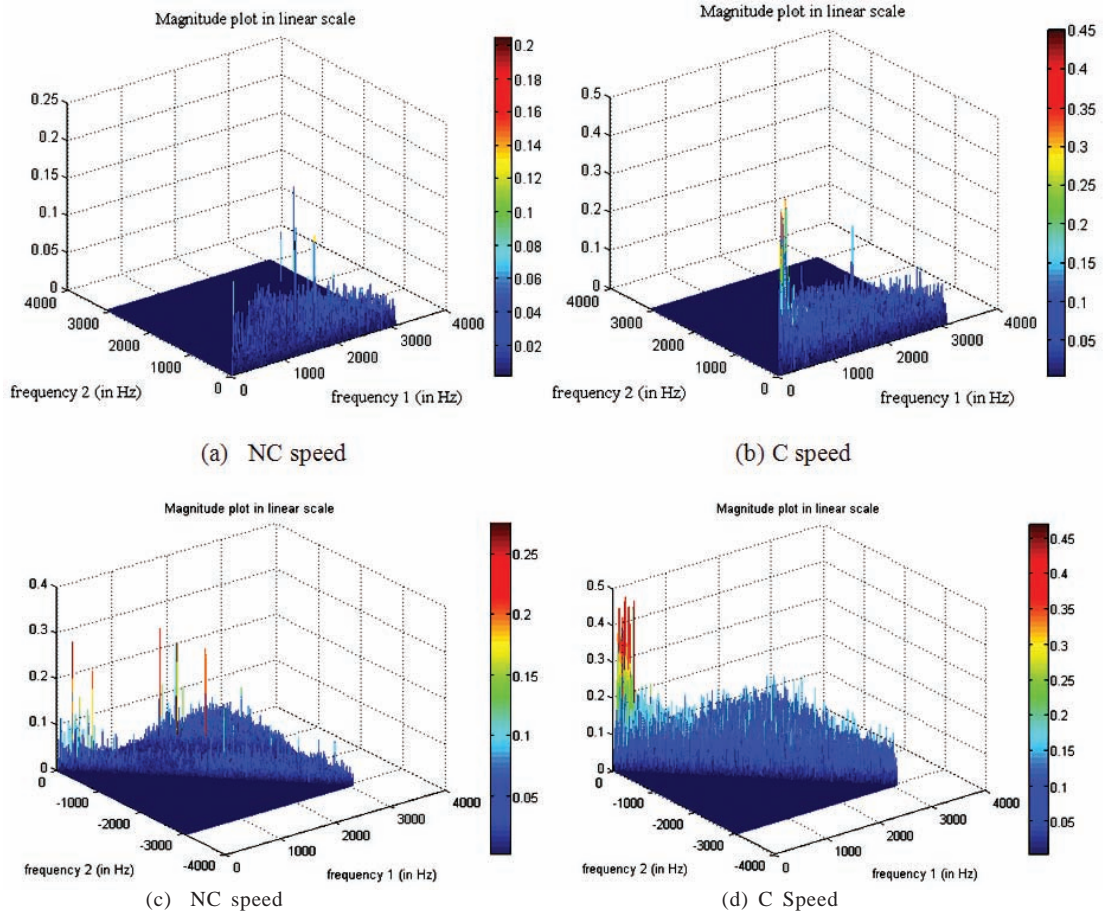


Figure 10. Bicoherence 0 - 3 KHz (a), (b) - sum components, (c), (d) - difference components.

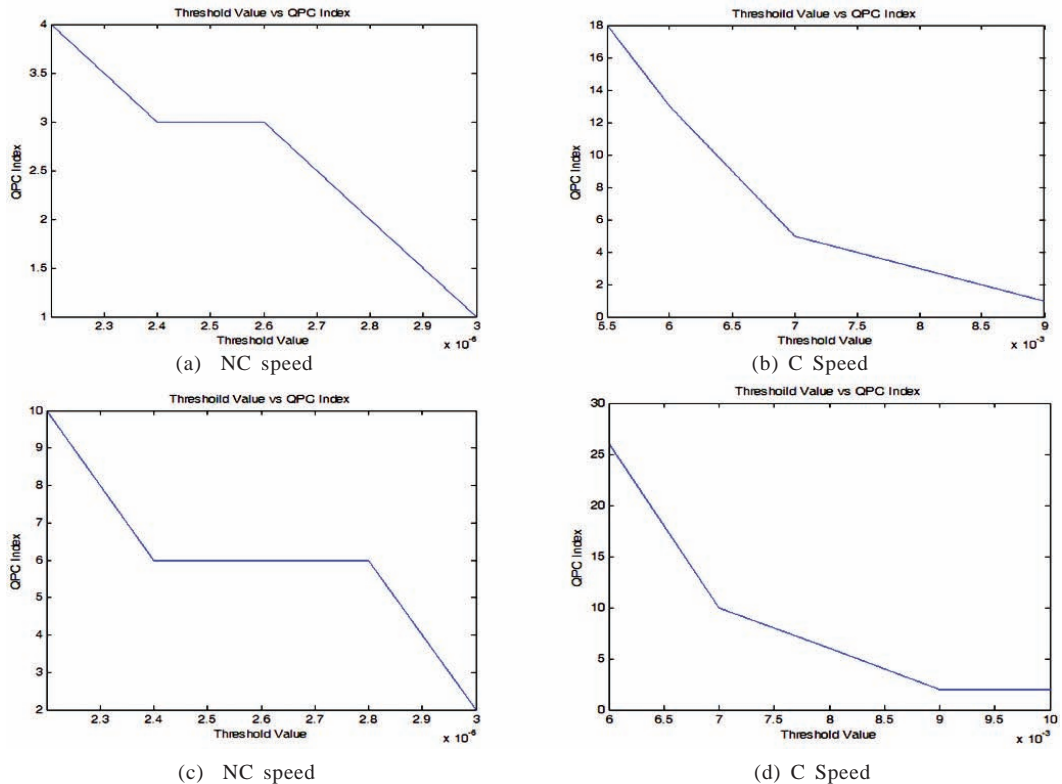


Figure 11. Plots of QPC Index vs threshold value computed from bispectrum data taken up to 1 KHz for sum components (a), (b) and difference components (c), (d).

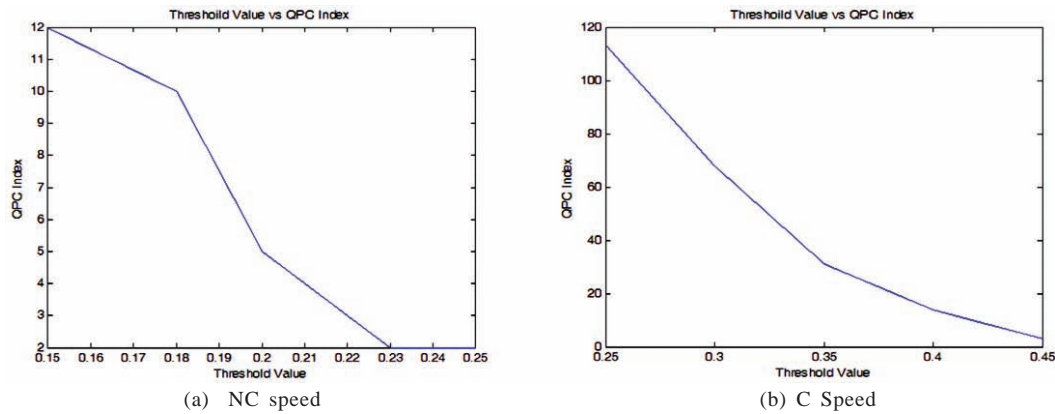


Figure 12. Plots of QPC Index vs threshold value computed from bicoherence data taken up to 3 KHz for difference components.

1 KHz. We observed an order of only 3.0 (approx.) increase in the strength from NC state to the C state of cavitation but an increase of the order of 7 approx. in QPC Index between the two states at minimum threshold value was observed. This indicates a significant increase in partially phase coupled components. QPC I_n increased 3 times at the maximum threshold value in contrast to that of sum components of bispectrum.

Similar results were obtained for the bispectrum and bicoherence analysis upto 1 KHz and up to 3 KHz for both the ‘sum’ and ‘difference’ components. The following are the results shown in the graphs:

Figures 11(a) to 11(d) show the result of bispectrum data analysis for sum and difference components up to 1 KHz. Figures 12(a) to 12(b) show result of bicoherence data analysis for sum and difference components up to 3 KHz. The following conclusions are inferred from these plots.

- i) In both cavitation states, QPC Index decreases monotonically as the threshold value is increased,
- ii) QPC Index increases significantly from NC to C state.

7. CONCLUSIONS

In the present study, underwater radiated noise data of ship measured by a hydrophone placed on the seabed has been used to understand propeller cavitation noise as a function of QPC Index. Distinguishable differences in the acoustic signature of a propeller with and without cavitation have been observed through the QPC Index. On the basis of analysis, the QPC Index concept presented here can be used to detect the fully developed cavitation. Future studies are being directed to find a relationship between propeller cavitation number and the QPC Index for a more quantitative description of propeller cavitation phenomenon.

REFERENCES

1. Tacconi, G.; Tesei, A. & Regazzoni, C.S. A New Host-based model for signal detection in non-Gaussian noise: An application to underwater acoustic communications. *IEEE* 1995, 620–625.
2. Lovik, A. Scaling of propeller cavitation noise. *Electronics Research Lab, The Norwegian Institute of Technology, Report No. STF-44-A80123. Feb 1980.*
3. Suslick, K.S.; Didenko, Y.; Fang, M.M.; Hyeon, T.; Kolbeck, K.J.; Mcnamara III, W.B.; Mdeleleni, M.M. & Wong, M. Acoustic cavitation and its chemical consequences. *Phil. Trans. Roy. Soc. A*, 1999,.
4. Leighton, T.G. The acoustic bubble. Academic Press, London, 1994.
5. Salvatore, F.; Testa, C. & Greco, L. Coupled Hydrodynamics - Hydroacoustics BEM modelling of marine propellers operating in a wake field. *In First International Symposium on Marine Propellers, Norway, June 2009.*
6. Brockett, P.L.; Melvin, H. & Gary, R.W. Nonlinear and non-Gaussian ocean noise. *J. Acous. Soc. Ame.*, 1987, **82**(4), 1386 – 1394.
7. Hinich, M.J.; Marandino, D. & Sullivan, E.J. Bispectrum of ship radiated noise. *J. Acous. Soc. Ame.*, 1988, **85**(4), 1512 – 1517.
8. Richardson, A.M & Hodgkiss, W.S. Bispectral analysis of underwater acoustic data. *J. Acous. Soc. Ame.*, 1994, **96**(2), 828 – 837.
9. Regazzoni, C.S.; Tesei, A. & Tacconi, G. A comparison between spectral and bispectral analysis for ship detection from acoustical time series. *IEEE*, 1994, II 282-89.
10. Haitao, Y.; Yingmin, W.; Zhanlin, X. & Wei, L. Feature extraction and classification based on bispectrum for underwater targets. *In International Conference on Intelligent System Design and Engineering Application 2010; IEEE Computer Soc.*; 742 – 745.
11. Srinivasan, K.; Panicker, P.; Raman, G.; Kim, B. & Williams, D.R. Study of coupled supersonic twinjets of complex geometry using higher-order spectral analysis. *J. Sound and Vibration.*, 2009, **323**, 910-931.
12. Urick, R.J. Principles of Underwater Sound. McGraw-Hill Book Company, New York, 1975
13. Nikiias, C.L. & Petropulu, A P. Higher-Order Spectra analysis. PTR Prentice Hall, New Jersey, 1993.
14. Sandhya, M.; Rajarajeswari, K. & Seetaramaiah, P. Detection and monitoring of propeller cavitation noise

using higher order spectral analysis. *In Proceedings of the International Conference on Recent Advances in Mathematical Sciences and Applications, Visakhapatnam, India, 2009.*

15. Subba Rao, T., & Gabr, M.M. A test for linearity of stationary time series. *J. Time Ser. Anal.*, 1980, 1(2), 145 -158.

CONTRIBUTORS



Mrs M. Sandhya received her BE (Electronics and Communications) from Andhra University and MTech (Radar and Communication) (Underwater Electronics) from IIT (Delhi) in 1990. Presently working as Additional Director at Naval Science and Technological Laboratory, DRDO, India. She has vast experience in the field of electronics of naval systems. Her research

areas of interest are : Underwater torpedoes, autonomous underwater vehicle, signal processing and embedded systems among others.



Prof. (Mrs) K. Rajarajeswari received her BE, ME and PhD in the field of Electronics and Communication. She is presently Principal, Viswanadha Institute of Technology And Management, College of Engg. She conducted several National and International Conferences of repute and guided more than 20 PhD scholars in the field of Signal Processing. Her

specialization is digital signal processing and wireless CDMA communication.



Prof. P. S. Ramaiah received his PhD in Computer Science and Systems Engineering from Andhra University in 1990. He is presently working as a Professor Emeritus in the department of Computer Science and Systems Engineering, Andhra University, Visakhapatnam. He has received DRDO's Academic Excellency Award for the year 2011. He has published 45 journal papers,

and presented 15 papers in international conference and 21 papers at national conferences. His areas of research include : Bio-electronics systems, safety-critical computing- software safety, VLSI and real time embedded systems.